

CHEMISTRY

A European Journal

A Journal of



Accepted Article

Title: Catalytic Type Excited-State N-H Proton Transfer Reaction in 7-Aminoquinoline and Its Derivatives

Authors: Kai-Hsin Chang, Ying-Hsuan Liu, Jiun-Chi Liu, Yu-Chiang Peng, Yu-Hsuan Yang, Zhi-Bin Li, Ren-Hua Jheng, Chi-Min Chao, Kuan-Miao Liu, and Pi-Tai Chou

This manuscript has been accepted after peer review and appears as an Accepted Article online prior to editing, proofing, and formal publication of the final Version of Record (VoR). This work is currently citable by using the Digital Object Identifier (DOI) given below. The VoR will be published online in Early View as soon as possible and may be different to this Accepted Article as a result of editing. Readers should obtain the VoR from the journal website shown below when it is published to ensure accuracy of information. The authors are responsible for the content of this Accepted Article.

To be cited as: *Chem. Eur. J.* 10.1002/chem.201904027

Link to VoR: <http://dx.doi.org/10.1002/chem.201904027>

Supported by
ACES

WILEY-VCH

Catalytic Type Excited-State N-H Proton Transfer Reaction in 7-Aminoquinoline and Its Derivatives

Kai-Hsin Chang,^{+[a]} Ying-Hsuan Liu,^{+[a]} Jiun-Chi Liu,^[a] Yu-Chiang Peng,^[b] Yu-Hsuan Yang,^[b] Zhi-Bin Li,^[b] Ren-Hua Jheng,^[b] Chi-Min Chao,^[b] Kuan-Miao Liu,^{*[b]} and Pi-Tai Chou^{*[a]}

Abstract: 7-Aminoquinoline (**7AQ**) and its various amino derivation (NR-H), including **Me-7AQ**, **Boc-7AQ**, **Ac-7AQ**, **Ts-7AQ** and **TFA-7AQ**, (**Scheme 1**), are strategically designed and synthesized to study their excited-state proton transfer (ESPT) properties. Due to the far separation between the proton donor NR-H and acceptor –N-sites, ESPT in **7AQ** derivatives, if available, should proceed with protic solvent catalysis process. As a result, assisted by methanol molecules, **Boc-7AQ**, **Ac-7AQ**, **Ts-7AQ** and **TFA-7AQ** undergo ESPT in methanol, while ESPT is prohibited in **Me-7AQ** and **7AQ**. ESPT is found to be influenced by acidity of NR-H and basicity of the proton-acceptor –N- in the quinoline moiety. The latter is varied by the NR-H substituent induced resonance effect to the quinoline –N-site. For those **7AQ** derivatives undergoing ESPT, the increase of quinoline basicity results in faster rate of ESPT, implying that the proton donation from methanol to the quinoline moiety may serve as a key step for ESPT. Studies also conclude the existence of equilibrium between cis- and trans- type NR-H in terms of its hydrogen bond (H-bond) configuration with methanol, in which only the cis- H-bonded form undergoes methanol assisted ESPT. Except for **TFA-7AQ**, the interconversion between cis- and trans-configurations is much faster than rate of ESPT, yielding amino- (normal form) and imine- (proton transfer tautomer) like emissions with distinct relaxation dynamics.

Introduction

Recently, via tuning the electronic property of the substituent –R on the NR-H proton donor that forms intramolecular hydrogen bond (H-bond) with the proton acceptor –N- group in the polycyclic heterocycles, both dynamics and thermodynamics of the excited-state intramolecular proton transfer (ESIPT) reaction can be harnessed by tuning the H-bonding strength.^[1–3] With the

same ESIPT core moiety, the results established an empirical relationship in that the stronger intramolecular H-bonding strength is, the fast and more exergonic is ESIPT. Varying the NR-H electronic property can even reach excited-state equilibrium between normal and proton-transfer tautomer states, so that the ratiometric emission for the normal versus the proton-transfer tautomer fluorescence can be fine-tuned, rendering white light generation.^[4]

In this study, for generalization, we lift the boundary of the unimolecular type ESIPT^[5–14] and extend the research to the systems where proton donor (NR-H) and acceptors are far separated without formation of intramolecular H-bond. Therefore, the occurrence of excited-state proton transfer (ESPT), if available, requires assistance of surrounding solvents.^[15–20] As for the –OH type of proton donor, a famous case in point should be ascribed to 7-hydroxyquinoline (**7HQ**, see **Scheme 1a**), in which the formation of a 2:1 (methanol: **7HQ**) H-bonded complex via solvent reorganization is required for ESPT.^[21–28] Studies of protic solvent molecules catalyzed ESPT may provide a valuable model to mimic the ubiquitous proton transfer reaction in bio-media.^[29–34]

Herein, we report the probe of methanol catalyzed ESPT for the 7-aminoquinoline (**7AQ**) derivatives, in which the –OH group of **7HQ** was substituted by various NR-H groups. One of the goals in this study is to probe the NR-H dependent ESPT reaction from amino- to imino- isomer (see **Scheme 1b**) by varying the electronic properties of the –R substituent. Unlike the intramolecular type ESPT, i.e., ESIPT, for which the relationship between H-bond strength and kinetics/thermodynamics can be probed (vide supra),^[1–3] **7AQ** derivatives lack the intramolecular H-bond and hence provide no available H-bond strength to access similar correlation. Alternatively, we intend to probe if there exists any relationship between solvent assisted ESPT and proton donor/acceptor sites. Accordingly, various **7AQ** derivatives **TFA-7AQ**, **Ts-7AQ**, **Ac-7AQ**, **Boc-7AQ**, and **Me-7AQ** were designed and synthesized, in which TFA, Ts, Ac, Boc and Me stand for trifluoroacetic, tosyl, acetyl, *tert*-butyloxycarbonyl and methyl groups, respectively (see **Scheme 1c**), to represent –R in the proton donating NR-H group. According to the –R electronic withdrawing strength, the acidity is expected to be in the order of **TFA-7AQ** > **Ts-7AQ** > **Ac-7AQ**, **Boc-7AQ** > **Me-7AQ**, which is also experimentally verified. Studies also show that the electronic properties of NR-H (and hence acidity) also influence the basicity of the proton-acceptor –N- in the quinoline moiety through the π -resonance effect. As a result, ESPT in terms of thermodynamics and kinetics, is governed by the interplay between proton donor and acceptor

[a] Kai-Hsin Chang, Ying-Hsuan Liu, Jiun-Chi Liu, Pi-Tai Chou
Department of Chemistry, National Taiwan University, Taipei, 10617
Taiwan, R.O.C.
E-mail: chop@ntu.edu.tw

[b] Yu-Chiang Peng, Yu-Hsuan Yang, Zhi-Bin Li, Ren-Hua Jheng, Chi-Min Chao, Kuan-Miao Liu
Department of Medical Applied Chemistry, Chung Shan Medical
University, Taichung 40201, Taiwan, R.O.C.
Department of Medical Education, Chung Shan Medical University
Hospital, Taichung 40201, Taiwan, R.O.C.
E-mail: lkm5688@gmail.com

[*] Kai-Hsin Chang and Ying-Hsuan Liu with equal contribution.

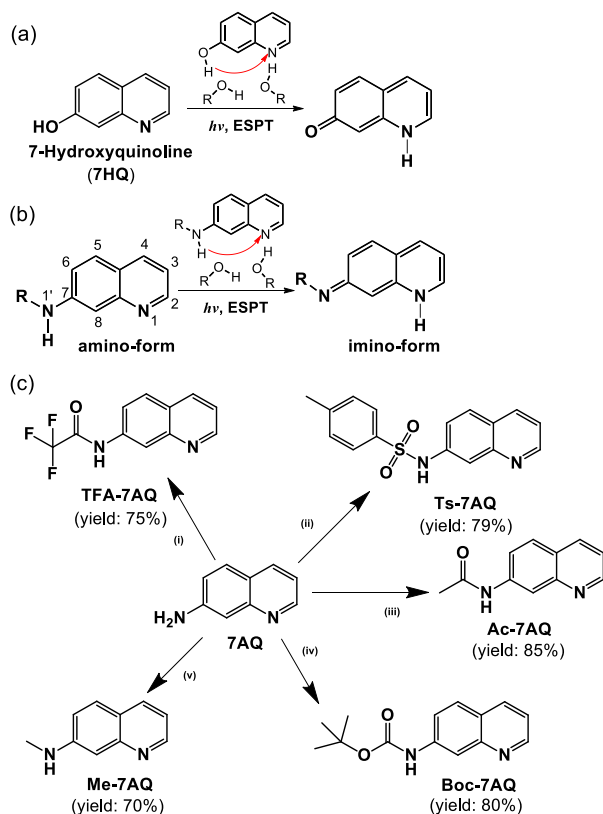
Supporting information for this article is given via a link at the end of the document.

FULL PAPER

sites. Detail of results and discussion is elaborated in the following sections.

Results and Discussion

Syntheses. The parent compound **7AQ** was synthesized from the reduction of 7-nitro-quinoline that could be obtained efficiently from the commercial available 1, 2, 3, 4-tetrahydroquinoline through nitration and dehydrogenation.^[35, 36] **TFA-7AQ**, **Ts-7AQ**, **Ac-7AQ** and **Boc-7AQ** were then synthesized from **7AQ** by a standard protocol to incorporate the corresponding protecting groups TFA-, Ts-, Ac- and Boc- respectively. **Me-7AQ** was obtained by refluxing **7AQ** with paraformaldehyde in basic methanol, followed by reduction with sodium borohydride.^[37] **DiMe-7AQ** was synthesized following the traditional reductive amination procedure. All studied compounds were purified and showed > 99% purity by ¹H-NMR and high resolution mass spectrometry (HRMS). Detailed



Scheme 1. (a) The proposed alcohol catalyzed ESPT reaction of **7HQ** derivatives. (b) The proposed alcohol catalyzed ESPT reaction of **7AQ** derivatives. Note that for (a) and (b) the alcohol molecules assisted ESPT is depicted in a qualitative manner. Detail of mechanism will be discussed later. (c) Synthetic routes from **7AQ** to various derivatives: (i) TFA, CH₂Cl₂; (ii) p-TsCl, pyridine, CH₂Cl₂; (iii) Ac₂O, CH₂Cl₂; (iv) Boc₂O, NaHMDS, THF; (v) PFA, NaOCH₃.

synthetic routes and the corresponding characterization are elaborated in the experimental section. The X-ray structure for one of the **7AQs**, **Ac-7AQ**, is shown in **Figure 1**, in which some informative bond distances and angles are denoted. Other crystal structures for **TFA-7AQ** and **Ts-7AQ** are shown in **Figure S1, S2** of supporting information (SI). In **Figure 1b**, two nitrogen atoms located at NR-H and quinoline moieties for **Ac-7AQ** are separated by 4.84 Å, which is too far to proceed with the intramolecular proton transfer. Note that in the crystal form **Ac-7AQ** favors a trans- configuration due to the lattice packing. Here, the cis- and trans- forms are defined as the NR-H hydrogen

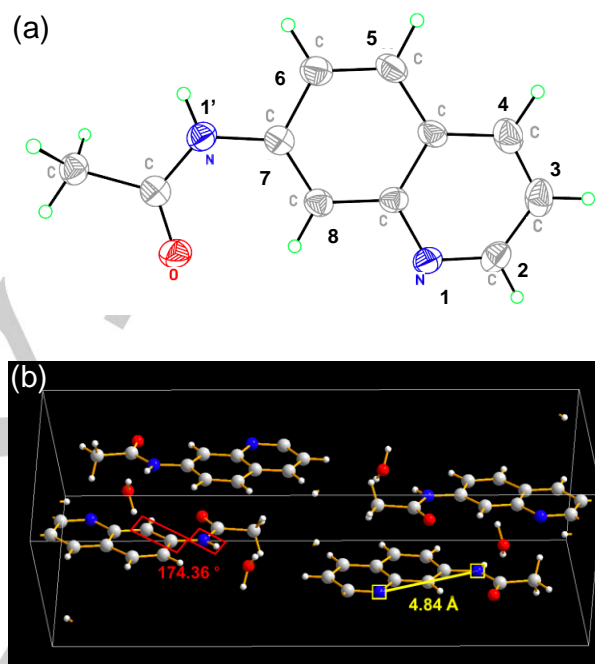


Figure 1. The X-ray structure of **Ac-7AQ** with thermal ellipsoids shown at the 50% probability. The distance between N(1), N(1') atoms and the dihedral angle $\theta = \angle \text{HN}(1')\text{-C}(7)\text{C}(8)$ (see **Scheme 1** for numbering) are 4.84 Å and 174.36°, respectively.

atom is located at the same and different side of the quinoline nitrogen, respectively, taking the dihedral angle $\theta = \angle \text{HN}(1')\text{-C}(7)\text{C}(8)$ as a reference. In this case, cis- and trans- forms are ascribed to $\theta = 0^\circ$ and 180° , respectively. In single crystal the structure of **Ac-7AQ** is in trans- configuration by realizing that $\angle \text{HN}(1')\text{-C}(7)\text{C}(8)$ are in 174.36° (see **Figure 1**). In methanol solvent, however, the cis- and trans- conformers, being hydrogen bonded by methanol molecules, are virtually in equilibrium (vide infra).

Photophysical properties. **Figure 2** shows the absorption and emission spectra of these **7AQ** derivatives in methanol. Clearly, **Me-7AQ** and **7AQ**, which are expected to possess the least and second least acidity among the studied **7AQ** derivatives, exhibit solely one emission band maximized at around 443 nm and 442 nm, respectively. The mirror image between absorption and emission spectra and regular Stokes shift of the emission peak wavelength infer lack of methanol solvent assisted ESPT. This

FULL PAPER

viewpoint is further affirmed by the observation of only normal emission band maximized at 430 and 419 nm for **Me-7AQ** and **7AQ**, respectively, in acetonitrile (see **Figure S3, S4**) where no protic solvent molecules could catalyze ESPT. In addition, **diMe-7AQ**, for which both N-H protons are replaced by the methyl groups to represent a non-proton transfer model, was synthesized (**Figure S5**). As a result, similar to **Me-7AQ** and **7AQ**, only one emission band was observed near 464 nm for **diMe-7AQ** in methanol (**Figure S5**). It is thus reasonable for us to conclude lack of methanol catalyzed ESPT in **Me-7AQ** and **7AQ**.

On the other hand, carrying electron withdrawing groups to increase the acidity of the proton donor, **Boc-7AQ**, **Ac-7AQ**, **Ts-**

7AQ and **TFA-7AQ** exhibit dual emissions in methanol, consisting of a higher-energy emission band (the F1 band) maximized around 365–375 nm and a lower-energy emission (the F2 band) with peak wavelengths at 540 nm, 560 nm, 580 nm and 582 nm for **TFA-7AQ**, **Ts-7AQ**, **Ac-7AQ**, and **Boc-7AQ**, respectively. In stark contrast, in aprotic solvents such as acetonitrile and dichloromethane, they all exhibit only one emission band at 450–500 nm (see **Figure S6**). The steady-state emission spectra thus clearly indicate the occurrence of ESPT for **Boc-7AQ**, **Ac-7AQ**, **Ts-7AQ** and **TFA-7AQ** catalyzed by the methanol molecules, forming an imine-like tautomer that exhibits the lower-energy F2 band at > 500 nm.

To gain further insight into the methanol catalyzed ESPT reaction in title **7AQs**, both absorption and fluorescence titration experiments were formed. **Figure 3a** shows the absorption titration spectra of **Boc-7AQ** titrated by methanol in cyclohexane. The formation of **Boc-7AQ/MeOH** H-bonded complexes can be clearly seen by the growth of a 350 nm shoulder throughout the titration. The **Boc-7AQ** H-bonded complex incorporating stoichiometric n MeOH molecules can be depicted as^[38, 39]



According to Benesi-Hildebrand derivation,^[38, 39] the equation for the titration can be expressed as follows

$$\frac{1}{(C_{\text{MeOH}})^n} = C_0 \epsilon_{350} K_a \frac{1}{A_{350}} - K_a \quad (2)$$

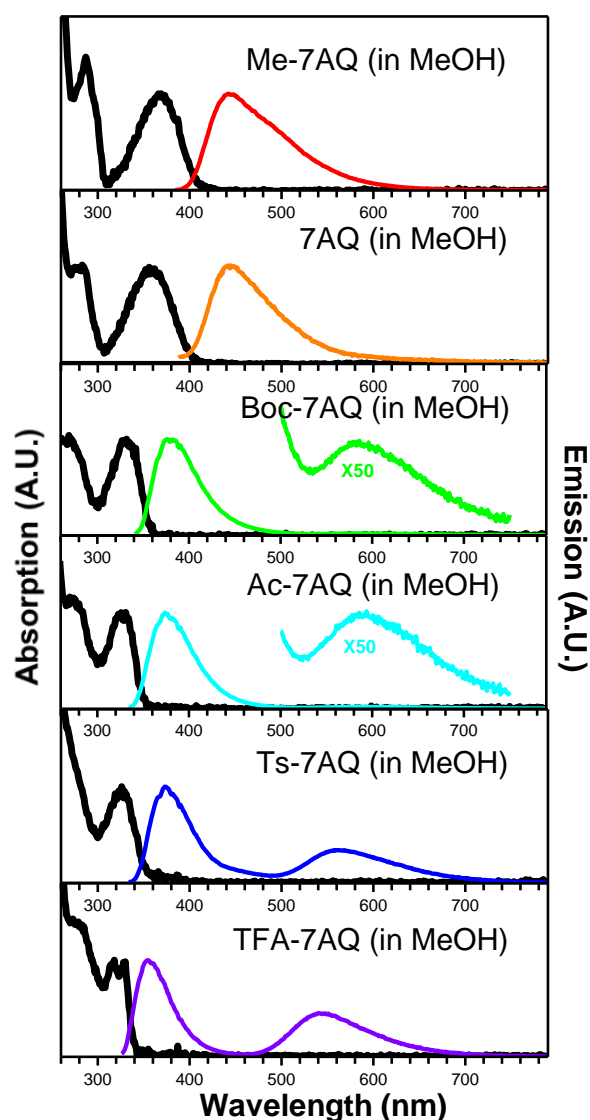


Figure 2. The absorption and emission spectra derivatives ($\sim 1.0 \times 10^{-5}$ M) in methanol. The excitation wavelength for the emission was at the peak wavelength of the lowest absorption band.

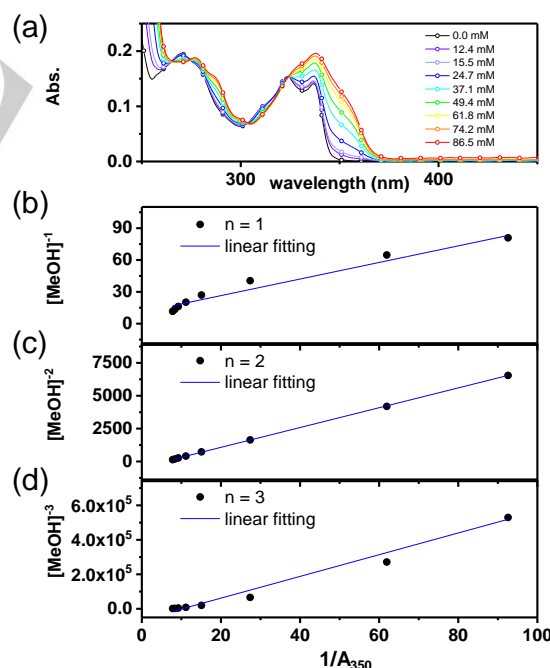


Figure 3. (a) The absorption spectrum of **Boc-7AQ** in cyclohexane by adding various MeOH concentration. (b) the plot of $1/C_{\text{MeOH}}^1$ against $1/A_{350}$. (c) the plot of $1/C_{\text{MeOH}}^2$ against $1/A_{350}$. (d) the plot of $1/C_{\text{MeOH}}^3$ against $1/A_{350}$.

FULL PAPER

where C_{MeOH} is concentration of methanol addition, n is the molar equivalent of methanol, C_0 is the concentration of **Boc-7AQ** in cyclohexane, ϵ_{350} is the absorption extinction coefficient at 350 nm, K_a is the equilibrium constant for the formation of H-bonded complex, A_{350} is the measured absorbance at 350 nm. **Figure 3(b)-3(d)** depict the plot of $1/(C_{MeOH})^n$ ($n = 1, 2$ and 3) as a function of $1/A_{350}$, which is expected to be linear under a specific stoichiometric number n for the complex formation. As a result, **Figure 3(c)** clearly indicates a linear fitting ($R^2 = 0.999$) for the plot of $1/(C_{MeOH})^2$ versus $1/A_{350}$, concluding the formation of a **Boc-7AQ**:methanol (1:2) H-bonded complex. K_a was then deduced to be $\sim 4 \times 10^2 M^{-2}$.

In yet another approach, the fluorescence titration experiment was also performed, in which the tautomer emission intensity, originating from the proposed **Boc-7AQ**:methanol H-bonded complex, as a function of methanol concentration. Similarly, base on Benesi-Hildebrand derivation,^[38, 39] the equation for the titration can be expressed in eq. (3)

$$\frac{1}{(C_{MeOH})^n} = \alpha C_0 \epsilon_{324} K_a \frac{1}{F_{580}} - K_a \quad (3)$$

where C_{MeOH} is concentration of methanol addition, n is equivalent of methanol, α is the instrument factor, C_0 is the concentration of **Boc-7AQ** in cyclohexane, ϵ_{324} is extinction coefficient at 324 nm which is the isosbestic point during the absorption titration, K_a is the equilibrium constant, F_{580} is the tautomer fluorescence intensity at 580 nm. As a result, **Figure 4(a)** depicts the tautomer emission spectra (F2) as a function of the added methanol concentration in cyclohexane. **Figure 4(b)-**

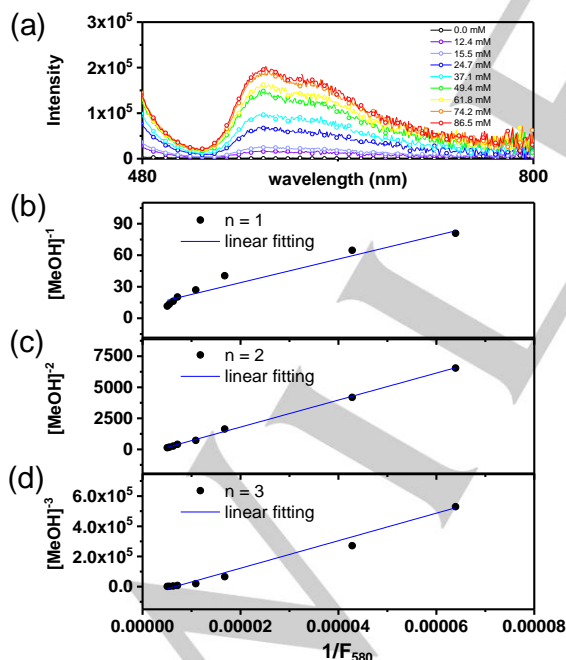


Figure 4. (a) The fluorescence spectrum of **Boc-7AQ** in cyclohexane by adding various MeOH concentration. (b) the plot of $1/C_{MeOH}^{-1}$ against $1/F_{580}$. (c) the plot of $1/C_{MeOH}^{-2}$ against $1/F_{580}$. (d) the plot of $1/C_{MeOH}^{-3}$ against $1/F_{580}$.

4(d) depicts the plot of $1/(C_{MeOH})^n$ ($n = 1, 2$ and 3) as a function of $1/F_{580}$, which is expected to be linear under a specific stoichiometric number n for the H-bonded complex formation. As a result, **Figure 4(c)** clearly indicates a linear fitting ($R^2 = 0.998$) for the plot of $1/(C_{MeOH})^2$ versus $1/F_{580}$. The result not only reaffirms the absorption titration study, concluding the formation of a **Boc-7AQ**:methanol (1:2) H-bonded complex. It also proves that ESPT originates from the **Boc-7AQ**:methanol (1:2) hydrogen bonded complex.

In an aim to probe the relationship regarding the acidity (proton donor) and basicity (proton acceptor), the pK_a values of NR-H and N⁺-H (quinoline nitrogen) for **7AQ** derivatives were measured by the pH-titration absorption spectrometry in aqueous solution (see **Table 1**, **Figure S7-S15**). As a result, the NR-H pK_a for **Me-7AQ** and **7AQ** was beyond the detection limit (> 14), while pK_a of **boc-7AQ** and **Ac-7AQ** was measured to be ~ 13.8 and ~ 13.2 , respectively. Relatively strong acidity was obtained for **Ts-7AQ** (pK_a 8.27) and **TFA-7AQ** (pK_a 8.13). Therefore, the pK_a values are in the order of **Boc-7AQ** > **Ac-7AQ** > **Ts-7AQ** > **TFA-7AQ**, inferring the increase of the NR-H acidity in a trend of **Boc-7AQ** < **Ac-7AQ** < **Ts-7AQ** < **TFA-7AQ**, which is in consistence with the increase of electron withdrawing strength.

Table 1. The pK_a of NR-H and N⁺-H (quinoline) for the studied **7AQs**

structure	NR-H	N ⁺ -H of quinoline
Me-7AQ	-	7.12
7AQ ^[40]	-	6.57
Boc-7AQ	~ 13.8	5.39
Ac-7AQ	~ 13.2	5.14
Ts-7AQ	8.27	4.70
TFA-7AQ	8.13	4.45

Interestingly, pK_a of the N⁺-H (quinoline nitrogen) is also varied by the NR-H substituents. According to the titration data (see **Table 1** and **Figures S7-S15**), pK_a of the N⁺-H is in a trend of **Me-7AQ** (7.12) > **7AQ** (6.57) > **Boc-7AQ** (5.39) > **Ac-7AQ** (5.14) > **Ts-7AQ** (4.70) > **TFA-7AQ** (4.45), so that the basicity of quinoline nitrogen is in the order of **Me-7AQ** > **7AQ** > **Boc-7AQ** > **Ac-7AQ** > **Ts-7AQ** > **TFA-7AQ**. Therefore, the stronger electron withdrawing strength $-R$ substituent (in NR-H) renders stronger NR-H acidity but weaker basicity of the quinoline nitrogen. The result may be expectable if one considers that NR-H and quinoline N sites are mutually interacted via the π -conjugation. On the one hand, the increase of the R- electron withdrawing ability increases the NR-H acidity. On the other hand, the resulted decrease of electron donating ability for the NR-H nitrogen decreases its resonance effect through π -conjugation to the quinoline nitrogen, and hence decreases the basicity of the quinoline nitrogen. We are aware that a better approach to correlate the excited-state phenomena should rely on the excited-state pK_a^* (* denotes the electronically excited state) that commonly assessed by the pH fluorescence titration. Unfortunately, the fluorescence of **7AQ** derivatives in aqueous

FULL PAPER

solution are too much complicated to be analyzed, consisting protonation, deprotonation and tautomerization in the excited state. Although pK_a and pK_a^* are very different, in theory, it is reasonable to assume the validity of a similar trend among same moieties, and hence pK_a will be used herein as a scale for the later discussion.

Time-resolved fluorescence. We then applied time-correlated single photon counting (TCSPC) technique to probe the fluorescence relaxation dynamics. In this study, the femtosecond light source (~100 fs) coupled with multichannel plates as the detecting system gives a system response time of ~25 ps, which is fast enough to resolve the methanol catalyzed ESPT kinetics in this study (vide infra). For **7AQ** and **Me-7AQ** where no proton-transfer tautomer (imine-like) emission is observed in the steady-state measurement (vide supra), the fluorescence kinetics, monitored at the normal emission peaks at 442 nm (**7AQ**) and 443 nm (**Me-7AQ**) are fitted to be single exponential with a lifetime of 0.48 ns and 4.86 ns, respectively. The much different population decay time can be rationalized by the quenching of the fluorescence via torsional motion along the RHN(1')-C(7) bond (see **Scheme 1** for numbering of carbon atom). Upon $\pi \rightarrow \pi^*$ excitation, the quinoline moiety becomes π -electron deficient. Therefore, the stronger electron donating property for HNMe in **Me-7AQ** (cf. NH_2 in **7AQ**) induces stronger resonance effect, forming partial HNMe=C double bond that restricts the torsional motion and hence reduces quenching of the emission. This viewpoint is further supported by the 2.6% and 25.1% emission quantum yield for **7AQ** and **Me-7AQ** in methanol, respectively. In other words, the RHN(1')-C(7) rotation quenching emission plays an important factor for the dynamics of excited-state relaxation, which are also evidenced by the studies of other **7AQ** derivatives, elaborated as follows.

Figure 5 shows the fluorescence kinetics of those **7AQ** derivatives showing ESPT properties in the steady-state measurement, so the emission dynamics can be monitored at both F1 (amino- form) and F2 bands (imine- form). Upon monitoring at the F1 band (**Figure 5(a)**), on the one hand, the kinetic traces for **Ac-7AQ**, **Boc-7AQ**, **Ts-7AQ** and **TFA-7AQ** all consist of two decay components. On the other hand, shown in **Figure 5(b)**, the F2 band reveals a long rise component from tens to few hundred picoseconds, followed by a long population decay. All pertinent data are listed in **Table 2**. Using **Boc-7AQ** as an example, upon monitoring at the F1 band (380 nm) the emission decay is fitted by two single exponential decay components with lifetime of 212 ps and 1.72 ns, while the F2 band is fitted to comprise a rise of 209 ps and a decay of 359 ps. The decay of 212 ps of the F1 band, within the experimental error of ± 10 ps, is identical with the rise of 209 ps of the F2 band, supporting a precursor-successor type of kinetic relationship. Note that for the methanol catalyzed ESPT of **7HQ**, which requires formation of stoichiometric 2:1 methanol:**7HQ** H-bonded complex, followed by H-bond reorganization and proton transfer, the rate of overall ESPT has been reported to be $\sim (170 \text{ ps})^{-1}$ [22,24]. Therefore, for **Boc-7AQ** it is reasonable to conclude the time constant of methanol assisted ESPT to be ~ 210 ps. Following

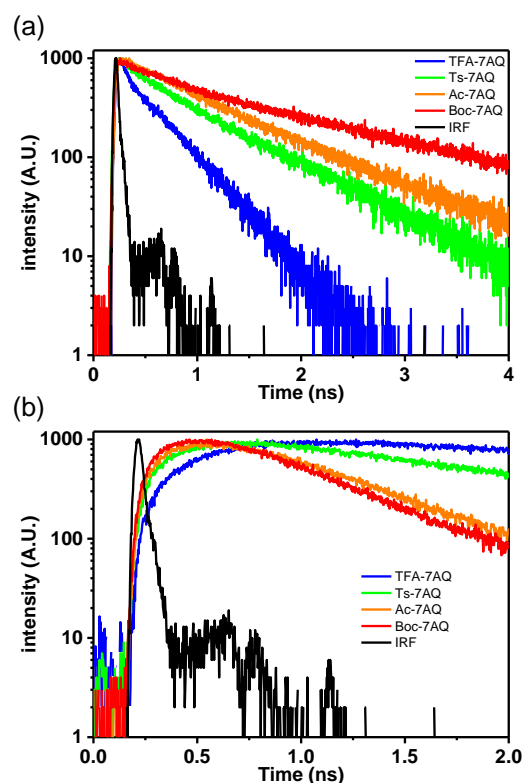


Figure 5. The fluorescence kinetics of **Boc-7AQ**, **Ac-7AQ**, **Ts-7AQ** and **TFA-7AQ** in methanol. The excitation wavelength: 310 nm. The emissions are monitored at peak wavelength (see **Table 2**) of the F1 band (a) and F2 band (b). IRF: instrument response function

ESPT, the resulted imine-like tautomer emission undergoes a population decay with a time constant of ~ 360 ps.

A remaining kinetic issue for **Boc-7AQ** is in regard to the origin of the fluorescence component with a 1.72 ns lifetime when monitoring at the F1 band. For the case of 7-hydroxyquinoline (**7HQ**) it has been well established that ESPT requires formation of stoichiometric 2:1 methanol:**7HQ** H-bonded complex, followed by the reorganization of these H-bonds relays and then proton transfer, to account for the overall rate of methanol catalyzed ESPT [24]. Due to the similar geometry (angle and distance) between proton donating and accepting sites, it is reasonable to expect that **7AQ** derivatives, if ESPT is available in methanol, should hold similar mechanism as that in **7HQ**, except for a distinct difference. Depending on the size and electronic properties of the -R group (in NR-H), we may expect to have different types of methanol/**7AQs** H-bonding configurations in the ground state, which are classified as trans- and cis- H-bonding configurations, the definition of which has been given in the early X-ray characterization section (vide supra). Shown in **Figure 6**, the trans-configuration, in which the NR-H proton donating site is too far away from the accepting -N- sites to form 2:1 (methanol: **7AQs**) H-bonded complex, requires rotation of the NR-H site along the RHN(1')-C(7) bond during the excited-

FULL PAPER

Table 2. The excited-state relaxation dynamics of 7AQ derivatives in methanol monitored by the rise and decay of the fluorescence at different wavelengths.

structure	QY (%)	normal form			tautomer form		
		monitored (nm)	τ_1 (ps)	τ_2 (ps)	monitored (nm)	τ_1 (ps)	τ_2 (ps)
Me-7AQ ^a	25.1	445	4860	-	-	-	-
7AQ ^a	2.6	450	477	-	-	-	-
Boc-7AQ ^b	14.2	380	212 (42.59%)	1724 (57.41%)	600	209 (-50.35%)	359 (49.65%)
Ac-7AQ ^b	9.6	380	216 (45.76%)	972 (54.24%)	600	213 (-50.77%)	481 (49.23%)
Ts-7AQ ^b	6.6	365	245 (46.00%)	841 (54.00%)	600	244 (-45.61%)	1418 (54.39%)
TFA-7AQ ^b	2.8	370	46 (56.96%)	370 (43.04%)	550	375 (-49.22%)	2877 (50.78%)

^a The excitation wavelength: 266 nm (8.2 MHz); ^b The excitation wavelength: 310 nm (82 MHz).

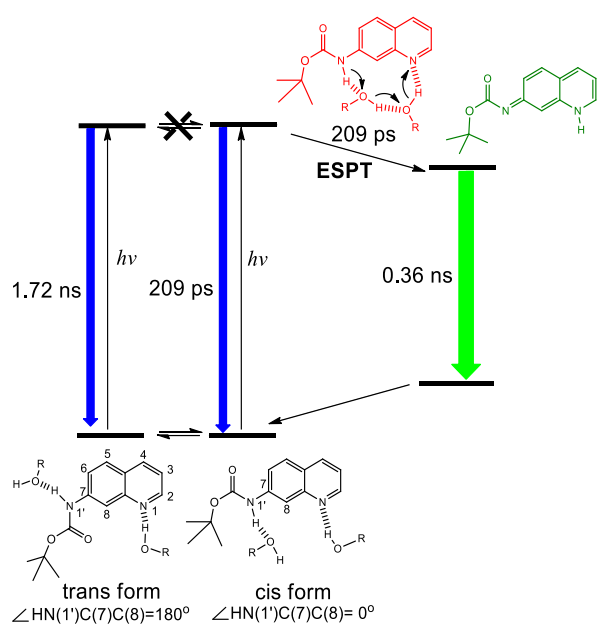


Figure 6. The proposed trans- and cis-type random H-bonding configurations using Boc-7AQ as an example. The dihedral angle is defined as $\theta = \angle \text{HN}(1')\text{C}(7)\text{C}(8)$. The cis and trans forms of 7AQs are ascribed to the structure with $\theta = \angle \text{HN}(1')\text{C}(7)\text{C}(8) = 0^\circ$ and $\theta = \angle \text{HN}(1')\text{C}(7)\text{C}(8) = 180^\circ$, respectively. Upon excitation, ESPT is prohibited in the trans-methanol hydrogen bonded complex, while the cis-methanol H-bonded complex undergoes methanol assisted ESPT via the formation of Boc-7AQ:methanol (1:2) cyclic H-bonding configuration (see structure in red).

state lifespan, forming the cis-configuration to proceed with ESPT. Therefore, the rotational dynamics along RHN(1')-C(7) play an important role for ESPT elaborated below.

Standing on the above viewpoint, the weak electron withdrawing -R group such as Boc- leads to stronger N- electron donating strength, endowing the BocHN(1')-C(7) bond with a partial double-bond-like character that inhibits the trans-cis rotation along the BocHN(1')-C(7) bond in the excited state. This explains the 1.72 ns component for the F1 emission band, which can be ascribed to the population decay time of the trans-configuration that does not undergo ESPT. Further support is given by the ratio of the pre-exponential value of ~1:1 for long (1.72 ns) versus short (212 ps) decay component monitored at the F1 band (380 nm, see Figure 5(a) and Table 2), indicating a

nearly equal distribution in the initial prepared trans- and cis- H-bond configurations. Theoretically, there should be no preference in population for either cis- or trans- configuration, considering a random H-bonding distribution between 7AQs and methanol solvents, giving a ~1:1 ratio for the trans- versus cis-configurations. Note that in this classification we neglect those non-planar H-bond configurations with respect to the quinoline moiety. This is because strong resonance effect should make RHN(1')-C(7) a double bond-like strength, which makes the HN(1')-R-C(7) plane nearly coplanar to the quinoline moiety. This viewpoint will be verified in the later theoretical approaches.

Due to similar electronic properties between acetyl (Ac-) and Boc- groups, the same interpretation can be applied to the Ac-7AQ for which the time constant of 216 ps and 0.97 ns (Table 2) monitored at the F1 normal emission band can be ascribed to the lifetime of cis- and trans- H-bond configured Ac-7AQ in methanol, respectively, in which the cis-configuration undergoes ESPT, while ESPT is prohibited in trans-configuration. Further support is given by the 213 ps rise component of the F2 imine-tautomer band (Table 2 and Figure 5(b)), which is identical with the decay of the fast component of the F1 band, showing a precursor-successor relationship caused by ESPT. As for Ts-7AQ, the tosyl group has stronger electron withdrawing than that of Boc- and Ac- groups, so that the (Ts)HN(1')-C(7) bond is subject to a more single bond-like rotation. However, the size of Ts- is significantly larger than Boc- and Ac-, which plays a counter effect to slow down the rotation. As a result, the 0.84 ns and 245 ps (Table 2) decay components resolved for the F1 band of Ts-7AQ are assigned to the lifetime of the trans- and cis-configurations, respectively, in which the cis-configuration undergoes methanol assisted ESPT, the time constant of which also well matches the rise time of the F2 band (244 ps).

As for TFA-7AQ, we expect the strongest electron withdrawing properties for TFA among the studied 7AQs. Therefore, the (TFA)HN(1')-C(7) bond is most probably a single bond like. This, together with its small size (cf. the Ts- group), should lead to a fast rotation along (TFA)HN(1')-C(7) bond. Experimentally, shown in Figure 5 and Table 2, two decay components of 46 ps and 369 ps are resolved for the F1 band of TFA-7AQ, in which 370 ps is nearly identical with the rise component of the F2 band (375 ps). Therefore, the time constant of ~370-375 ps attributed to ESPT seems to be unambiguous. This makes the assignment of 46 ps to the decay time constant of the trans-configuration interesting, which indicates that the rate of trans-cis

FULL PAPER

interconversion is faster than that of ESPT. In other words, kinetically, one can consider a pre-equilibrium between trans-cis configuration, followed by the methanol assisted ESPT from the cis-configuration. For this case, the kinetic derivation depicted in the supporting information (see **Scheme S1**, and **eq. (27)**, **(28)**, **(30)**, **(31)**) indicates that the normal emission (F1 band) of trans-configuration should exhibit a fast decay time constant, which is the reciprocal of sum of the forward and reverse conversion rate constants and is experimentally measured to be 46 ps. Moreover, both cis- and trans- configurations undergo the same population decay time of 370 ps. In other words, both configurations contribute to the F2 band. The imine tautomer (F2 band) that originates from ESPT of the cis-configuration has corresponding rise time of 375 ps, followed by a population decay time of 2.88 ns. The derived kinetic expression thus well explains the experimental results.

Theoretical approach Prior to discussing the structure-ESPT relationship for **7AQs**, computational studies were carried out in an aim to gain insight into the thermodynamics of ESPT. Early absorption and emission titration experiments have concluded the formation of a **7AQs**:methanol (1:2) hydrogen bonded complex that is required for ESPT. We then performed the calculation the thermodynamics of ESPT based on **7AQs**: methanol (1:2) hydrogen bonded complex. In this approach, the geometry of the ground state was optimized by the density functional theory (DFT). The excited-state structures and the related optical properties were calculated with time-dependent density functional theory (TDDFT) methodology with a CAM-B3LYP hybrid function.^[41, 42, 43] The 6-31+G(d,p) basis set was employed for all atoms. Both calculations for ground and excited state are incorporated with a polarizable continuum model (PCM)^[44] in methanol. The results are showed in **Table S1** of the supporting information. **Table S1** also lists the calculated absorption (normal) and emission (normal and tautomer) energy in terms of wavelength (nm), which, is comparable with the experimental data despite a trend of blue shift for all calculated **7AQs**. Note that the applied CAM-B3LYP hybrid function commonly results in higher energy.^[43, 45]

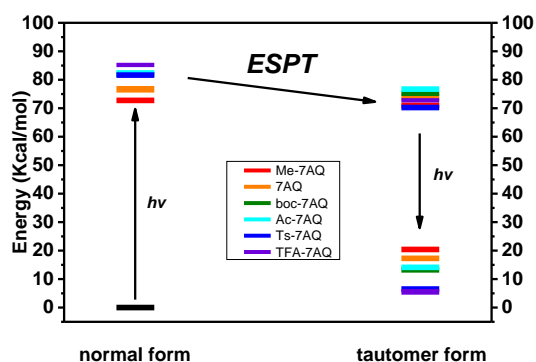


Figure 7. The relative energies between normal and proton-transfer tautomer in ground and in the first singlet excited states for **7AQs**. In this plot, we intentionally set the ground state of each **7AQ** derivative to be zero.

Clearly, the calculated ΔE (the free energy difference between normal and tautomer forms in the S_1 state) is in the order of **TFA-7AQ** (-12.4 kcal/mol) < **Ts-7AQ** (-12.3 kcal/mol) < **Boc-7AQ** (-6.7 kcal/mol) < **Ac-7AQ** (-5.7 kcal/mol) < **7AQ** (-2.7 kcal/mol) < **Me-7AQ** (-2.0 kcal/mol) (**Figure 7**). Although the results cannot reflect the prohibition of ESPT in **7AQ** and **Me-7AQ**, their trend in exegonicity of ESPT for the title **7AQs** is consistent with the experimental results.

Also, the calculation of the energy required for interconversion between cis- and trans- form in the ground as well as the lowest lying singlet excited states was performed. Due to the complexity of the solvent hydrogen bonding structures, for which the computation approach is formidable at current stage, we instead calculated the energy of cis- to trans- conversion by scanning dihedral angle θ in every 10° for **7AQs**, while the solute-solvent interaction is based on the polarizable continuum model (PCM).^[44] In the ground state, the results (see **Figure 8** and below) show a trend of cis-to-trans barrier in the order of **TFA-7AQ** (1.9 kcal/mol) \approx **Ts-7AQ** (1.9 kcal/mol) < **Ac-7AQ** (2.4 kcal/mol) < **Boc-7AQ** (2.9 kcal/mol). This small value, together with near isoenergetics between cis- and trans- forms, allows the thermally activated interconversion between cis- and trans- configurations in the ground state, as confirmed by the

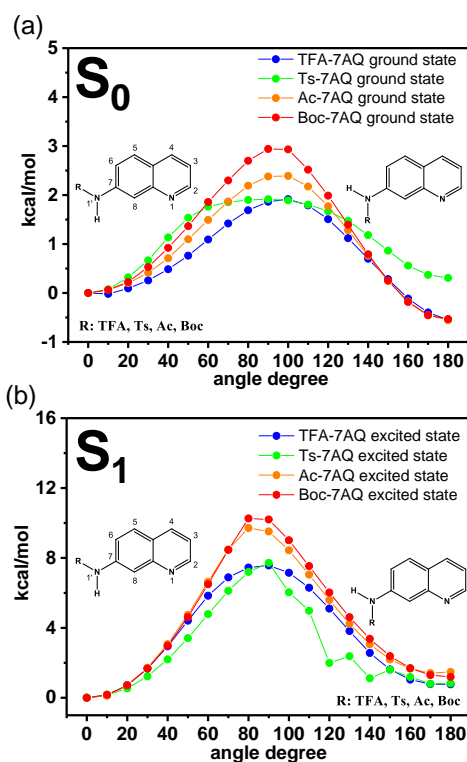


Figure 8. The calculated energy for various **7AQs** as a function of the dihedral angle $\theta = \angle \text{HN}(1')\text{C}(7)\text{C}(8)$ by scanning θ in every 10° in (a) the ground state and (b) the lowest lying singlet excited state in methanol, in which the surrounding methanol solvents are treated by the polarizable continuum model. Note that $\theta = 0^\circ$ and 180° are ascribed to cis- and trans- forms, respectively.

FULL PAPER

experimental observation. Also, the calculation (see **Figure 8(a)**) clearly indicates the existence of equilibrium between cis- and trans- forms in the ground state. This is expectable because both cis- and trans- forms are subject to the same solvation environment.

Upon electronic excitation, the energy difference between optimized cis- and trans- forms was also calculated in the S_1 state. The result shown in (**Figure 8(b)**) also supports the similar energy between trans- and cis- configuration. In sharp contrast, however, despite the similar trend of **TFA-7AQ** (7.6 kcal/mol) < **Ts-7AQ** (7.7 kcal/mol) < **Ac-7AQ** (9.7 kcal/mol) < **Boc-7AQ** (10.3 kcal/mol) (see **Figure 8(b)**), the magnitude of rotational barrier for the cis-trans conversion in the S_1 state is significantly larger than that of the ground state. The result manifests the influence of RHN(1')-C(7) resonance induction in the excited state, giving more RHN(1')-C(7) double bond character (cf. ground state) that hinders the rotation. Due to the lack of information on the specific methanol H-bond configuration and viscosity influence, the rate of interconversion was not accessible. However, the large barrier obtained for **Ac-7AQ** (9.7 kcal/mol) and **Boc-7AQ** (10.3 kcal/mol) support the inhibition of the cis/trans- interconversion in the excited state, while the smallest barrier of 7.6 kcal/mol for **TFA-7AQ**, together with its

small size (cf. **Ts-7AQ**), infers feasible cis-/trans- interconversion, in a qualitative manner.

In the NR-H type of excited-state intramolecular proton transfer (ESIPT), conclusion has been drawn in that the stronger is the intramolecular H-bond, the faster is the rate of ESIPT.^[1,2] As for **7AQs** the lack of intramolecular H-bond forbids us to probe relevant correlation. Thus, instead of the use of H-bonding strength, we would like to probe if ESPT kinetics, similar to the above thermodynamic relationship, can be drawn based on the acidity of **7AQs**; that is, the more acidic is NR-H, the faster the ESPT kinetics is for **7AQs**. Accordingly, a plot of the rate of methanol assisted ESPT as a function of pK_a for those **7AQs** exhibiting ESPT is shown in **Figure 9(a)**. To our surprise, on the contrary, the result indicates that the more acidic is NR-H, the slower the ESPT kinetics is for **7AQs**. For example, **TFA-7AQ** is the most acidic among the studied **7AQs** whereas its ESPT time constant of 375 ps is slower than 208 ps of **Boc-7AQ** that has the least acidity among the ESPT **7AQs**. On the other hand, alternatively, an attempt was also made by plotting the rate of ESPT for **7AQs** as a function of the basicity of quinoline nitrogen, for which the higher pK_a of $-NH^+$ indicates lower conjugated $-N-$ base (**Figure 9(b)**). The results show that the higher basicity is the quinoline $-N-$, the fast rate of ESPT is for **7AQs**. Thus, on the one hand, the trend of ESPT thermodynamics correlates with the electron donating-withdrawing ability and hence the acidity of NR-H. That is, the more acidic is the NR-H of **7AQs** the more exergonic is ESPT. On the other hand, the rate of ESPT increases as increasing the quinoline $-N-$ basicity, implying that the proton donation to the quinoline $-N-$ site may serve as a rate determining step for methanol catalyzed ESPT in **7AQs**.

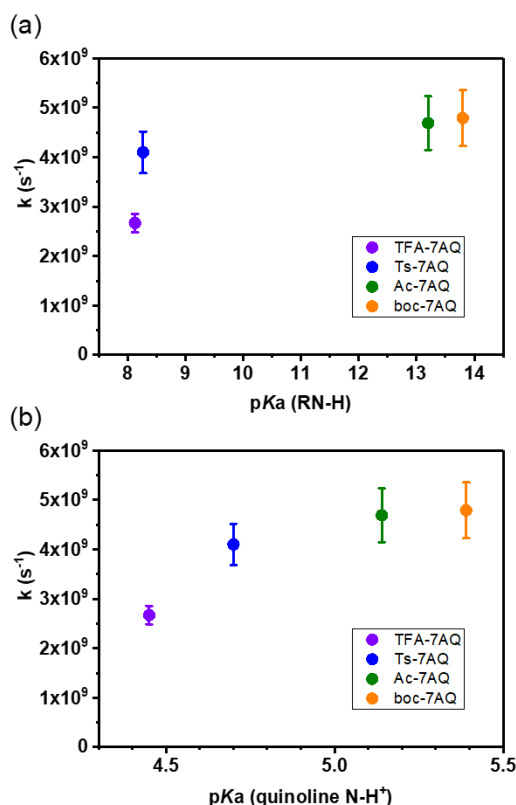


Figure 9. (a) The plot of rate constant for ESPT of **7AQs** as a function of the NR-H acidity in pK_a . (b) The rate constant for ESPT of **7AQs** as a function of the pK_a of $-NH^+$ (quinoline nitrogen). The rate constants were obtained by fluorescence dynamics and pK_a values were measured via pH titration experiment.

Conclusions

In conclusion, a comprehensive photophysical study has been carried out on a new class of amino-type ESPT compounds **7AQs** with an aim of shedding light on the protic solvent (methanol) assisted ESPT reaction. Using **Boc-7AQ** as an example, the excited-state relaxation mechanism is clearly depicted in **Figure 6**. In methanol, both cis- and trans- forms of **Boc-7AQ** are in equilibrium and they exhibit identical absorption spectra. On the one hand, upon exciting the trans form, due to a large energy barrier, the trans-to-cis conversion is prohibited during the lifespan in the excited state. Therefore, the excited trans- form gives a long population lifetime of 1.72 ns. On the other hand, the excitation of the cis- form undergoes methanol assisted ESPT with an overall time constant of 209 ps, which is the time required to achieve a **Boc-7AQ**:methanol (1:2) cyclic hydrogen bonded complex (see **Figure 6**, structure in red) and execute proton transfer, giving rise to a normal and a tautomer emission with a lifetime of 209 ps and 360 ps, respectively. Except for **TFA-7AQ** the interconversion between cis- and trans- configurations in the excited state is inhibited due to the large barrier created by the partial RHN(1')-C(7) double-bond character via the resonance induction effect. Experimentally, ESPT for **Me-7AQ** and **7AQ** is thermally unfavorable, but is allowed in **Boc-7AQ**, **Ac-7AQ**, **Ts-7AQ** and **TFA-7AQ**.

FULL PAPER

Different from previously published N-H intramolecular H-bonded molecules undergoing ES IPT,^[1,2] **7AQs** do not possess intramolecular H-bond. Therefore, the previously established correlation among H-bond strength, ES IPT kinetics and ES IPT thermodynamics cannot be applied. Nevertheless, for **7AQs** the results show that the more acidic is the NR-H the more exergonic is ESPT whereas the rate of ESPT increases as increasing the quinoline -N- basicity. The latter may infer that the rate determining step for methanol catalyzed ESPT lies in the proton donation to the quinoline -N- site.

Experimental Section

All reactions were carried out in oven- or flame-dried glassware under a positive pressure of argon. All reagents and solvents were purchased commercially and used without further purification. TLC was performed on Merck 5735 DC-plastikfolien Kieselgel 60 F254 precoated plates. Flash column chromatography was performed on silica gel (Merck 7736 Kieselgel 60H). ¹H and ¹³C NMR spectra were recorded on Bruker AVIII or Varian Unity-400 MHz spectrometers in CDCl₃, or d₆-DMSO. The chemical shifts were reported in δ ppm relative to the internal standard. HRMS data was obtained from a Waters LCT Premier XE (ESI-TOF/MS) and FOEL JMS-HX110. HR-FAB mass spectra and HR-EI mass spectra were conducted on a JMS-700 double focusing mass spectrometer (JEOL, Tokyo, Japan) with a resolution of 8000(3000) (5% valley definition). The FT-IR spectra were recorded on a Bomen-MB-100 FT-IR spectrometer.

7-Nitro-1, 2, 3, 4-tetrahydroquinoline. 1, 2, 3, 4-tetrahydroquinoline (5.305 g, 39.8 mmol) was added dropwise into conc. H₂SO₄ (15 mL) in an ice bath. After stirring for 30 mins, it was added dropwise the mixture of conc. HNO₃ (3 mL) in conc. H₂SO₄ (8 mL) and stirred at 0°C for another 3 hrs. The result was poured into ice water and neutralized to pH = 6 with Na₂CO_{3(aq)}. After filtration, the filtrate was extracted with EtOAc (3 x 20 mL). The organic layer was dried over anhydrous MgSO₄, concentrated, and purified by silica column chromatography (EtOAc/Hexanes 1:10) to afford the title compound (3.920 g, 55% yield) as orange oil. ¹H-NMR (400 MHz, d₆-DMSO, ppm) δ = 7.26 (s, 1H), 7.21 (dd, J = 8.2, 2.4 Hz, 1H), 7.05 (d, J = 8.0 Hz, 1H), 6.40 (s, 1H), 3.22 (t, J = 6.4 Hz, 2H), 2.74 (t, J = 6.4 Hz, 2H), 1.79 (m, 2H). HRMS (EI, m/z): calcd for (C₉H₁₁N₂O₂)⁺: 179.0815; Found: 179.0809.

7-Nitroquinoline. To a solution of 7-nitro-1, 2, 3, 4-tetrahydroquinoline (500 mg, 1.94 mmol) in CH₂Cl₂ (60 mL) was added DDQ (879.5 mg, 3.88 mmol) and the mixture was stirred for 30 mins. The solid was removed and the filtrate was extracted with CH₂Cl₂ (3 x 20 mL) followed by washing with brine. The combined organic extracts were dried over anhydrous MgSO₄. After filtration and concentration under reduced pressure, the residue was purified by silica chromatography (EtOAc/Hexanes 1:5) to afford **7-nitroquinoline** (312 mg, 92%) as yellow oil. ¹H-NMR (400 MHz, d₆-DMSO, ppm): δ = 9.10 (dd, J = 4.0, 1.2 Hz, 1H), 8.80 (s, 1H), 8.57 (d, J = 8.4 Hz, 1H), 8.33 (dd, J = 5.4, 2.4 Hz, 1H), 8.26 (d, J = 8.8 Hz, 1H), 7.76 (dd, J = 8.4, 2.0 Hz, 1H). HRMS (EI, m/z): calcd for (C₉H₇N₂O₂)⁺: 175.0508; Found: 175.0513.

7-Aminoquinoline (7AQ). A suspension of SnCl₂ (4.355 g, 22.97 mmol) in conc. HCl (35 mL) was added to a solution of 7-nitro-quinoline (1 g, 5.74 mmol) in acetic acid (17.5 mL). The mixture was heated at 70°C for 30 mins and then allowed to cool to room temperature. The mixture was treated with 10% NaOH_(aq) to pH = 12 and then extracted with CH₂Cl₂ (3 x 10 mL). The combined organic extracts were dried over anhydrous

MgSO₄. After filtration and concentration under reduced pressure, the residue was purified by silica chromatography (EtOAc/Hexanes 1:5) to afford **7AQ** (691 mg, 83%) as brown solid. ¹H-NMR (400 MHz, d₆-DMSO, ppm): δ = 8.55 (dd, J = 4.0, 1.6 Hz, 1H), 7.98 (dd, J = 8.0, 1.6 Hz, 1H), 7.57 (d, J = 8.4 Hz, 1H), 7.04 (dd, J = 8.0, 4.4 Hz, 1H), 6.96 (dd, J = 8.4, 2.0 Hz, 1H), 6.90 (d, J = 2.0 Hz, 1H), 5.73 (2H, s). HRMS (EI, m/z): calcd for (C₉H₉N₂)⁺: 145.0760; Found: 145.0754.

2,2,2-Trifluoro-N-(quinolin-7-yl)acetamide (TFA-7AQ). To a solution of **7AQ** (162 mg, 1.12 mmol) in CH₂Cl₂ (5 mL) was added 2,2,2-trifluoroacetic acid (190 μL, 1.35 mmol) and the mixture was stirred at room temperature for 16 hrs. The result was neutralized carefully with 10% NaOH_(aq) and then extracted with CH₂Cl₂ (3 x 10 mL). The combined organic extracts were dried over anhydrous MgSO₄ and the filtrate was concentrated. The residue was purified by silica chromatography (EtOAc/Hexanes 1:3) to afford **TFA-7AQ** (204 mg, 75% yield) as white solid. ¹H NMR (400 MHz, CDCl₃, ppm) δ = 8.91 (dd, J = 4.4, 1.6 Hz, 1H), 8.44 (brs, 1H), 8.23 (d, J = 1.6 Hz, 1H), 8.14 (dd, J = 8.4, 1.6 Hz, 1H), 7.88 (dd, J = 8.8, 2.0 Hz, 1H), 7.85 (d, J = 8.8 Hz, 1H), 7.40 (dd, J = 8.4, 4.4 Hz, 1H). ¹³C NMR (100 MHz, d₆-DMSO, ppm) δ = 155.2, 144.5, 142.0, 141.3, 130.6, 122.3, 121.7, 115.3, 115.0, 95.1 ppm. IR (KBr, cm⁻¹) 3213, 2993, 1716, 1630, 1566, 1504, 1466, 1441, 1394, 1319, 1279, 1204, 1151, 841, 753. HRMS (EI, m/z): calcd for C₁₁H₈N₂OF₃ (M+H)⁺: 241.0589; Found: 241.0589.

4-Methyl-N-(quinolin-7-yl)benzenesulfonamide (Ts-7AQ). To a solution of **7AQ** (100 mg, 0.69 mmol) in pyridine (2 mL) was added *p*-toluenesulfonyl chloride (158 mg, 0.83 mmol) and the mixture was stirred at room temperature for 16 hrs. The solution was neutralized carefully with 10% HCl_(aq) and extracted with CH₂Cl₂ (3 x 10 mL). The combined organic extracts were dried over anhydrous MgSO₄. After filtration and concentration under reduced pressure, the residue was purified by silica chromatography (CH₃OH/CH₂Cl₂ 1:50) to afford **Ts-7AQ** (165 mg, 79% yield) as yellow solid. ¹H-NMR (400 MHz, d₆-DMSO, ppm): δ = 10.73 (s, 1H), 8.75 (d, J = 4.0 Hz, 1H), 8.18 (d, J = 8.0 Hz, 1H), 7.81 (d, J = 8.8 Hz, 1H), 7.70 (d, J = 8.0 Hz, 2H), 7.61 (s, 1H), 7.37-7.29 (m, 4H), 2.26 (s, 3H). ¹³C NMR (100 MHz, d₆-DMSO, ppm) δ = 151.1, 148.1, 143.5, 138.9, 136.9, 135.6, 129.8, 126.7, 124.4, 120.3, 120.1, 115.6, 20.9 ppm. IR (KBr, cm⁻¹) 3062, 2873, 1626, 1579, 1510, 1450, 1362, 1323, 1158, 1091, 972, 836, 663. HRMS (FAB, m/z): calcd for C₁₆H₁₅N₂O₂S (M+H)⁺: 299.0854; Found: 299.0854.

N-(Quinolin-7-yl)acetamide (Ac-7AQ). To a solution of **7AQ** (165 mg, 1.14 mmol) in CH₂Cl₂ (5 mL) was added acetic anhydride (162 μL, 1.72 mmol) and the mixture was stirred at 70°C for 10 hrs. The reaction solution was neutralized carefully with 10% NaOH_(aq) and extracted with CH₂Cl₂ (3 x 10 mL). The combined organic extracts were dried over anhydrous MgSO₄. After filtration and concentration under reduced pressure, the residue was purified by silica chromatography (CH₃OH/CH₂Cl₂ 1:50) to afford **Ac-7AQ** (181 mg, 85% yield) as white solid. ¹H NMR (400 MHz, d₆-DMSO, ppm) δ = 10.28 (s, 1H), 8.80 (d, J = 4.4 Hz, 1H), 8.38 (s, 1H), 8.23 (d, J = 8.0 Hz, 1H), 7.87 (d, J = 8.4 Hz, 1H), 7.67 (d, J = 8.8 Hz, 1H), 7.37 (dd, J = 8.0, 4.0 Hz, 1H), 2.10 (s, 3H). ¹³C NMR (100 MHz, d₆-DMSO, ppm) δ = 169.0, 150.7, 148.4, 139.5, 135.9, 128.5, 125.2, 120.8, 120.0, 116.7, 24.6 ppm. IR (KBr, cm⁻¹) 3052, 3012, 2345, 1675, 1623, 1586, 1545, 1500, 1458, 1435, 1370, 1353, 835. HRMS (FAB, m/z): calcd for C₁₁H₁₁N₂O (M+H)⁺: 187.0871; Found: 187.0876.

tert-Butyl quinolin-7-ylcarbamate (Boc-7AQ). To a solution of **7AQ** (500 mg, 3.47 mmol) in anhydrous THF (10 mL) was added NaHMDS (3.81 mL, 7.63 mmol, 2M in THF) at room temperature under nitrogen atmosphere. The mixture was stirred for 15 mins and then *di-tert*-butyl dicarbonate (794 mg, 3.64 mmol) in anhydrous THF (5 mL) was added dropwise into the solution. The reaction mixture was stirred overnight

FULL PAPER

after which time the solvent was removed under reduced pressure. The residue was diluted with water and extracted with EtOAc (3 x 15 mL). The combined organic extracts were dried over anhydrous MgSO₄. After filtration and concentration under reduced pressure, the residue was purified by silica chromatography (EtOAc/Hexanes 1:1) to afford **Boc-7AQ** (680 mg, 80%) as white solid. ¹H-NMR (400 MHz, d₆-DMSO, ppm) δ = 9.74 (1H, s), 8.77 (dd, *J* = 4.4, 1.6 Hz, 1H), 8.21-8.17 (m, 2H), 7.83 (d, *J* = 8.8 Hz, 1H), 7.63 (dd, *J* = 8.8, 2.0 Hz, 1H), 7.34 (dd, *J* = 8.4, 8.0 Hz, 1H), 1.50 (s, 9H). ¹³C-NMR (100 MHz, CDCl₃, ppm) δ = 152.8, 151.0, 148.9, 139.9, 136.0, 128.8, 124.9, 120.0, 119.9, 115.6, 81.3, 28.6 ppm. IR (KBr, cm⁻¹) 3212, 2993, 1726, 1630, 1565, 1505, 1466, 1441, 1394, 1286, 1117, 842, 754. HRMS (EI, *m/z*): calcd for C₁₄H₁₇N₂O₂ (M+H)⁺: 245.1290; Found: 245.1281.

N-Methylquinolin-7-amine (Me-7AQ). To a mixture of **7AQ** (50 mg, 0.34 mmol) and sodium methoxide (94 mg, 1.73 mmol) in methanol (5 mL) was added the methanol solution (1 mL) of paraformaldehyde (14 mg, 0.47 mmol). After refluxing for 12 hrs, sodium borohydride (13 mg, 0.34 mmol) was added and stirred for another 2 hrs. The solvent was then removed under reduced pressure and the residue was extracted with CH₂Cl₂ (3 x 5 mL) and washed with water. The combined organic extracts were dried over anhydrous Na₂SO₄. After filtration and concentration under reduced pressure, the residual solid was purified on aluminium oxide (CH₂Cl₂ as eluent) to give **Me-7AQ** (37 mg, 70% yield) as yellow liquid. ¹H NMR (400 MHz, CDCl₃, ppm) δ = 8.71 (dd, *J* = 4.4, 2.0 Hz, 1H), 7.94 (dd, *J* = 8.0, 1.6 Hz, 1H), 7.54 (d, *J* = 8.8 Hz, 1H), 7.09 (dd, *J* = 8.0, 4.4 Hz, 1H), 7.02 (d, *J* = 2.4 Hz, 1H), 6.89 (dd, *J* = 8.4, 2.0 Hz, 1H), 4.13 (brs, 1H), 2.95 (d, *J* = 4.8 Hz, 3H). ¹³C NMR (100 MHz, CDCl₃, ppm) δ = 150.5, 150.4, 150.1, 135.6, 128.4, 121.7, 118.4, 117.2, 104.4, 30.5 ppm. IR (KBr, cm⁻¹) 3326, 3246, 3058, 2929, 1904, 1725, 1623, 1536, 1464, 1400, 1356, 1321, 1279, 1220, 1147, 1061, 973, 945, 824, 764, 667. HRMS (EI, *m/z*): calcd for (C₁₀H₁₀N₂)⁺: 158.0844; Found: 158.0849.

N,N-Dimethylquinolin-7-amine (diMe-7AQ). A mixture of **7AQ** (62 mg, 0.43 mmol), paraformaldehyde (136 mg, 2.16 mmol) and sodium cyanoborohydride (136 mg, 4.32 mmol) in acetic acid (3 mL) was stirred at room temperature for 22 hrs. 25% NaOH(aq) was added to neutralize the acetic acid. The mixture was extracted with CH₂Cl₂ (3 x 10 mL) and washed with water. The combined organic extracts were dried over anhydrous Na₂SO₄. After filtration and concentration under reduced pressure, the residual solid was purified on silica gel (CH₃OH/CH₂Cl₂ 1:60) to give **diMe-7AQ** (50 mg, 67% yield) as yellow liquid. ¹H NMR (400 MHz, CDCl₃, ppm) δ = 8.71 (dd, *J* = 4.4, 1.6 Hz, 1H), 7.94 (dd, *J* = 8.0, 1.6 Hz, 1H), 7.62 (d, *J* = 8.8 Hz, 1H), 7.19-7.12 (m, 2H), 7.08 (dd, *J* = 8.0, 4.4 Hz, 1H), 3.08 (s, 6H). ¹³C NMR (100 MHz, CDCl₃, ppm) δ = 151.0, 150.4, 149.9, 135.3, 128.2, 120.8, 117.1, 116.1, 106.7, 40.4 ppm. IR (KBr, cm⁻¹) 3378, 2925, 2854, 2806, 1935, 1719, 1622, 1510, 1438, 1357, 1240, 1151, 1064, 969, 823, 763, 663, 613. HRMS (EI, *m/z*): calcd for C₁₁H₁₂N₂⁺: 172.1000; Found: 172.0998.

Spectroscopic measurement.

Steady-state absorption spectra were recorded using Hitachi U-3310 spectrophotometer, emission spectra were measured by Edinburgh FS920 fluorometer. Picosecond time-resolved studies were performed with an Edinburgh FL 900 TCSPC system with femtosecond oscillator (Tsunami, Spectra-Physics) with a central output wavelength at 800 nm. The polarization was set at a magic angle (54.7°) with respect to the pump polarization direction to eliminate anisotropy. The excitation light source of 266 nm is generated from 800 nm of Tsunami by β-barium metaborate (β-BBO). The pKa measurements were performed with pH meter (PH-500) that was corrected by buffer solution (phosphate) pH7 and pH4 (Fisher Chemical).

Acknowledgements

P.-T. C. thanks for the financial support by Ministry of Science and Technology (MOST), featured areas research program within the framework of the Higher Education Sprout Project administrated by Ministry of Education (MOE) of Taiwan. We are grateful to the National Center for the High-performance Computing (NCHC) of Taiwan for the valuable computer time and facilities.

Conflict of interest

The authors declare no conflict of interest.

Keywords: ESPT • proton transfer • 7-aminoquinoline • Protic Solvent Catalyzed Excited-State Proton Transfer

References

- [1] C. L. Chen, Y. T. Chen, A. P. Demchenko, P. T. Chou, *Nat. Rev. Chem.* **2018**, *2*, 131-143.
- [2] H. W. Tseng, J. Q. Liu, Y. A. Chen, C. M. Chao, K. M. Liu, C. L. Chen, T. C. Lin, C. H. Hung, Y. L. Chou, T. C. Lin, T. L. Wang, P. T. Chou, *J. Phys. Chem. Lett.* **2015**, *6*, 1477-1486.
- [3] G. J. Zhao, K. L. Han, *Acc. Chem. Res.* **2011**, *45*, 404-413.
- [4] I. E. Serdiuk, *J. Phys. Chem. C* **2017**, *121*, 5277-5286.
- [5] P. K. Sjnngupta, and M. Kasha, *Chem. Phys. Lett.* **1979**, *68*, 382-385.
- [6] T. P. Smith, K. A. Zaklika, *J. Am. Chem. Soc.* **1991**, *113*, 4035-4036.
- [7] A. Ranganathan, G. U. Kulkarni, *J. Phys. Chem. A* **2002**, *106*, 7813-7819.
- [8] M. M. Henary, Y. Wu, J. Cody, S. Sumalekshmy, J. Li, S. Mandal, C. J. Fahmi, *J. Org. Chem.* **2007**, *72*, 4784-4797.
- [9] A. I. Ciuciu, K. Skonieczny, D. Koszelewski, D. T. Gryko, L. Flamigni, *J. Phys. Chem. C* **2013**, *117*, 791-803.
- [10] A. J. Stasyuk, M. K. Cyrański, D. T. Gryko, M. Solà, *J. Chem. Theory Comput.* **2015**, *11*, 1046-1054.
- [11] Q. Wang, L. Xu, Y. Niu, Y. Wang, M. S. Yuan, Y. Zhang, *Chem. Asian J.* **2016**, *11*, 3454 - 3464.
- [12] T. Mutai, T. Ohkawa, H. Shono, K. Araki, *J. Mater. Chem. C* **2016**, *4*, 3599-3606.
- [13] S. D. Glover, G. A. Parada, T. F. Markle, S. Ott, L. Hammarström, *J. Am. Chem. Soc.* **2017**, *139*, 2090-2101.
- [14] M. Shahida, A. Misrab, *J. Photochem. Photobiol., A* **2017**, 190-199.
- [15] M. Kasha, *J. Chem. Soc., Faraday Trans. 2* **1986**, *82*, 2379-2392.
- [16] T. Nakagawa, S. Kohtani, M. Itoh, *J. Am. Chem. Soc.* **1995**, *117*, 7952-7957.
- [17] J. Waluk, *Acc. Chem. Res.* **2003**, *36*, 832-838.
- [18] G. Wiosna-Satyga, Y. Nosenko, M. Kijak, R. P. Thummel, B. Brutschy, Jacek Waluk, *J. Phys. Chem. A* **2010**, *114*, 3270-3279.
- [19] O. H. Kwon, O. F. Mohammed, *Phys. Chem. Chem. Phys.* **2012**, *14*, 8974-8980.
- [20] K. Kerdpol, R. Daengngern, J. Meeprasert, S. Namuangruk, N. Kungwan, *Theor. Chem. Acc.* **2016**, *135*, 208.
- [21] S. F. Mason, J. Philp, B. E. Smith, *J. Chem. Soc. A* **1968**, 3051-3056.

FULL PAPER

- [22] P. J. Thistlethwaite, P. J. Corkill, *Chem. Phys. Lett.* **1982**, *85*, 317-321.
- [23] M. Itoh, T. Adachi, K. Tokumura, *J. Am. Chem. Soc.* **1983**, *105*, 4828-4829.
- [24] J. Konijnenberg, G. B. Ekemans, A. H. Huizer, A. G. O. Varma, *J. Chem. Soc., Faraday Trans. 2* **1989**, *85*, 39-51.
- [25] P. T. Chou, S. S. Martinez, *Chem. Phys. Lett.* **1995**, *235*, 463-470.
- [26] H. J. Park, O. H. Kwon, C. S. Ah, D. J. Jang, *J. Phys. Chem. B* **2005**, *109*, 3938-3943.
- [27] O. H. Kwon, Y. S. Lee, B. K. Yoo, D. J. Jang, *Angew. Chem. Int. Ed* **2006**, *45*, 415-419.
- [28] S. Y. Park, Y. S. Lee, O. H. Kwon, D. J. Jang, *Chem. Commun.* **2009**, 926-928.
- [29] P. Ball, *Chem. Rev.* **2008**, *108*, 74-108.
- [30] X. Shu, P. Leiderman, R. Gepshtein, N. R. Smith, K. Kallio, D. Huppert, S. J. Remington, *Protein Science* **2007**, *16*, 2703-2710.
- [31] K. Y. Chung, Y. H. Chen, Y. T. Chen, Y. H. Hsu, J. Y. Shen, C. L. Chen, Y. A. Chen, P. T. Chou, *J Am Chem Soc.* **2017**, *139*, 6396-6402.
- [32] D. Stoner-Ma, A. A. Jaye, K. L. Ronayne, J. r. Nappa, S. R. Meech, P. J. Tonge, *J. Am. Chem. Soc.* **2008**, *130*, 1227-1235.
- [33] C. Fang, R. R. Frontiera, R. Tran, R. A. Mathies, *Nature*, **2009**, *462*, 200-205.
- [34] M. Chatteraj, B. A. KING, G. U. Bublitz, S. G. Boxer, *Proc. Natl. Acad. Sci. U. S. A.* **1996**, 8362-8367.
- [35] A. Cordeiro, J. Shaw, J. O'Brien, F. Blanco, I. Rozas, *Eur. J. Org. Chem.* **2011**, 1504-1513.
- [36] E. A. Braude, R. P. Linstead, *J. Chem. Soc.* **1954**, 3544-3547.
- [37] J. Barluenga, A. M. Bayon, G. Asensio, *J. Chem. Soc., Chem. Commun.* **1984**, 1334-1335.
- [38] M. L. Benesi, J. H. Hildebrand, *J. Am. Chem. Soc.* **1949**, *71*, 2703-2707.
- [39] P. T. Chou, C. Y. Wei, C. -R. C. Wang, F. T. Hung, C. P. Chang, *J. Phys. Chem. A* **1999**, *103*, 1939-1949.
- [40] S. G. Schulman, K. Abate, P. J. Kovi, A. C. Capomacchia, D. Jackman, *Analytica Chimica Acta.* **1973**, *65*, 59-67.
- [41] A. Becke, *Phys. Rev. A*, **1988**, *38*, 3098-3100.
- [42] C. Lee, W. Yang, R. Parr, *Phys. Rev. B*, **1988**, *37*, 785-789.
- [43] T. Yanai, D. P. Tew, N. C. Handy, *J. Chem. Phys. Lett.* **2004**, *393*, 51-57.
- [44] S. Miertuš, E. Scrocco, J. Tomasi, *Chem. Phys.* **1981**, *55*, 117-129.
- [45] I. H. Nayyar, *J. Phys. Chem. C* **2013**, *117*, 18170-18189.